

Mechanical Effect on Gene Transfection Based on Dielectric Elastomer Actuator

Chao Gao,¹ Zhichao Li,¹ Jiang Zou,¹ Jin Cheng, Kai Jiang, Changrun Liu, Guoying Gu,* Wei Tao,* and Jie Song*

Cite This: *ACS Appl. Bio Mater.* 2020, 3, 2617–2625

Read Online

ACCESS |

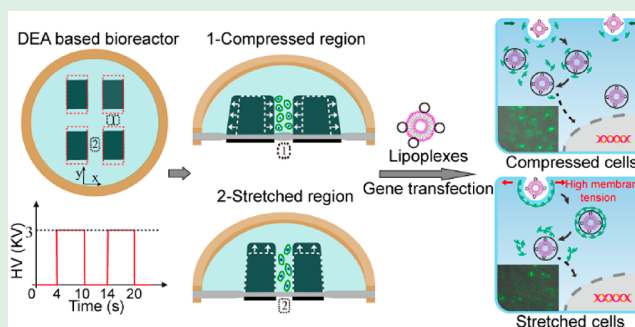
Metrics & More

Article Recommendations

Supporting Information

ABSTRACT: Gene transfection has been widely applied in genome function and gene therapy. Although many efforts have been focused on designing carrier materials and transfection methods, the influence of mechanical stimulation on gene transfection efficiency has rarely been studied. Herein, dielectric elastomer actuator (DEA)-based stimulation bioreactors are designed to generate tensile and contractile stress on cells simultaneously. With the example of the EGFP transfection, cells with high membrane tension in the stretching stimulation regions had lower transfection efficiency, while the transfection efficiency of cells in the compressing regions tended to increase. Besides, the duty cycle and loading frequency of the applied stress on cells were also important factors that affect gene transfection efficiency. Furthermore, the pathways of cell endocytosis with the effect of mechanical stimulation were explored on the mechanism for the change of EGFP transfection efficiency. This design of the DEA-based bioreactor, as a strategy to study gene transfection efficiency, could be helpful for developing efficient transfection methods.

KEYWORDS: DEA-based bioreactor, mechanical stimulation, membrane tension, transfection efficiency, cell endocytosis



1. INTRODUCTION

Gene transfection, a technique that transports biologically functional nucleic acids (e.g., DNA, antisense oligonucleotide, and RNA interference) into cells and maintains their biological functions, has been broadly applied in the study of gene expression regulation,¹ gene function,² drug screening,³ and gene therapy.^{4–6} Gene transfection requires certain transfection reagents to transport the target gene into cells, and the entire transfection process needs to overcome extracellular and intracellular obstacles, including the plasma membrane, the cytoskeletal framework in the cytoplasm, and nuclear envelope, which have great influence on the DNA endocytosis, trafficking, and entry into the nucleus, respectively.^{7–9} However, due to blood flow, muscle contraction, and respiration, cells are in a dynamic microenvironment *in vivo* and stimulated by a multimechanical model, such as shear, stretching and contractile stress,^{10,11} so dynamic microenvironment is also an important factor affecting gene transfection efficiency. Thus, studying the effects of mechanical stimulation on gene transfection is useful to further explore the gene function and gene therapy techniques.

Because of the hindrance of cell membranes, the transmembrane ability of exogenous nucleic acids is an important factor affecting the efficiency of gene transfection.⁷ Nowadays, common methods to improve the efficiency of gene transfection mainly focus on the development of carrier materials

and delivery methods such as chemical methods (e.g., cationic liposomes, calcium phosphate, and nanoparticles),^{12–14} viral methods (e.g., viral vector),^{15,16} and physical methods (e.g., microinjection, electroporation).^{17,18} Although these methods have greatly improved the success rate and efficiency of genes entering into cells, there is still a series of technical problems, such as high cytotoxicity, high technical difficulty, and biological safety, that limits their applications in human treatment and other fields. In contrast to the studies on the design of gene vectors and transfection methods, scholars have noticed the effect of cell morphology on gene transfection efficiency, which provided a research idea for the development of efficient and safe gene transfection methods.¹⁹ Meanwhile, studying the effects of mechanical stimulation on cell endocytosis is also an important factor to influence gene transfection efficiency.^{20–25} Previous works focused on the mechanism of the effect of cell membrane tension on endocytosis by means of mechanical stretch and hypo-osmotic treatment,^{9,26–33} but the detailed effect of different mechanical

Special Issue: Nucleic Acids: Chemistry, Nanotechnology, and Bioapplications

Received: December 21, 2019

Accepted: January 20, 2020

Published: January 28, 2020



stimulation on gene transfection was not mentioned such as stretching and compressing stimulations. The main reason is that traditional stimulation methods, such as motor drive and pneumatic device, are generally complex in structure and large in size, making it difficult to combine real-time dynamic observation with microscope perfectly.³⁴ Thus, reasonable design of cell mechanical stimulation devices is a prerequisite for the study of the effect of mechanical stimulation on gene transfection efficiency.

In this work, DEA-based bioreactors were designed to demonstrate the effects of stretching and compressing stimulation on cell endocytosis and expression of plasmid DNA (pDNA) *in vitro*. Specifically, we designed a DEA-based driving system composed of a cell culture device and a bidirectional driven DEA-based bioreactor. The advantages of the DEA-based driving system were that both tensile and contractile stress could be generated on the same membrane, and all mechanical stimulation regions were optically transparent. In addition, the DEA-based system could be compatible with the optical microscope, which was convenient to observe the cell state in real time. As a proof of concept, pDNA was chosen to study the differences of A549 cells transfection efficiency between the stretched and compressed regions. Specifically, the effects of mechanical loading parameters on cell endocytosis and gene transfection were explored such as loading frequency, tensile ratio, and duty cycle. Moreover, factors affecting transfection efficiency by mechanical stimulation were preliminary analyzed.

2. MATERIALS AND METHODS

2.1. DEA-Based Deformable Bioreactor Design and Fabrication. An organic silicone membrane (Wacker ELASTOSIL Film) was used as dielectric elastomer material due to its low viscosity elasticity, rapid response speed, and heat resistance. First, the silicone membrane was prestretched as demonstrated in previous research.^{34–36} Moreover, a larger prestretch was applied in the x axis ($\lambda_x = 2.6$, $\lambda_y = 1.2$) to generate uniaxial movement. Then the prestretched membrane was fixed on a laser cutting poly(methyl methacrylate) (PMMA) frame with high temperature-resistant tape to support the prestretch of the membrane, and the PMMA frame was processed by laser cutting with 25 mm inner diameter and 5 mm height for storing cell culture medium. Another function of the polymethyl metal frame was to fix the wire to the positive electrode. A four-electrode DEA was designed to realize the visualization of stretching and compression deformation on a membrane simultaneously. In detail, the lower surface of the membrane was covered with four electrodes and connected to the positive electrode of the high voltage power supply. Considering the aseptic requirements of cell growth environment, the upper surface of the membrane was directly connected to the negative electrode with the culture medium instead of being coated with carbon electrodes.

In particular, we attempted to cover the silver electrode on the surface of the dielectric-elastomer membrane with uniform thickness by means of vacuum evaporation. Before vacuum evaporation, a corresponding mask was designed according to the shape of the electrodes; the mask was made of poly(methyl methacrylate) and processed by laser cutting. The evaporation current was about 100 A, and evaporation rate was less than 0.2 Å/s. It is particularly important to note that the direction of the mask electrode should be parallel to the direction of the membrane prestretch and should not have an angle crossing. Because of the low stiffness and good conductivity at large deformation,³⁷ carbon-based materials are commonly used as electrode material. In this work, carbon-based electrodes were used to study the effect of mechanical stimulation on cell transfection efficiency. In the direction of electrodes movement, the spacing between two electrodes has great influence on the electrode stretching

characteristics, so we designed four different spacings (1 mm, 1.5 mm, 2 mm, 2.3 mm) and analyzed the stretching characteristics of these electrodes. The width of electrode (L_1) was 1 mm. To optimize the influence of the fixed boundary condition, the dimension of the prestretched membrane was ten-times larger than that of the electrodes in y axis.^{35,38}

Circular DEA was fixed on a designed cell culture device, which was processed by 3D-printing. The cell culture device consisted of an external mixed gas tank and a heating unit, which provided the necessary environmental conditions (37 °C, 5% CO₂) for cell culture. A ring heating unit was adopted to ensure the uniform distribution of temperature in the culture device. We designed two different sizes of cell culture devices, one with small size to cooperate perfectly with the microscope and realize the real-time imaging observation of the cell stimulation process. The other was a high-throughput cell incubator unit allowing carry out of four groups of cell transfection tests at the same time, which was mainly used to study the effect of mechanical stimulation on gene transfection efficiency.

2.2. Performance Characterization of DEA-Based Bioreactor. The deformation was observed by inverted microscope (IX 71, Olympus), and the unilateral strain deformation in y axis of each electrode was ΔL , so we could obtain the average tensile strain as $2\Delta L/L_1$ and the average compression strain as $2\Delta L/L_2$. We should mention that the above calculation process can only obtain the average strain of the region; considering the instability of electro-mechanical tension, the deformation distribution of the membrane was measured using Ncorr, which is an open source digital image correlation (DIC) tool that can obtain objects deformation and strain fields based on image analysis.³⁹

2.3. Cell Preparation. A549 (Human lung carcinoma cell line) was purchased from the cell bank of the Chinese Academy of Sciences (Shanghai, People's Republic of China) and selected to study the effect of mechanical loading on the efficiency of gene transfection and expression. pEGFP-N1 plasmid was amplified in *Escherichia coli* DH5 α competent cells (Sangon Biotech, Shanghai, China), extracted and purified by UNIQ-500 Column Endotoxin-Free Plasmid Max-Preps Kit (Sangon Biotech, Shanghai, China) according to the manufacture instruction. Before seeding, it was necessary to pretreat and improve the biocompatibility of the DEA-based bioreactor. First of all, the DEA-based bioreactor was sterilized with 75% ethanol, and then the bioreactor was activated by ultraviolet-light for 1 h. Finally, the membrane was incubated with human fibronectin (5 $\mu\text{g}/\text{cm}^2$, 1 mL) in phosphate buffered saline (PBS) for 2 h at room temperature to improve the biocompatibility of the membrane and increase the cell adhesion ability. The A549 cells were incubated on the surface of the membrane and filled with the cell culture medium, and the bioreactor was kept in the cell culture incubator at 37 °C with 5% CO₂ and a 95% humidified atmosphere. Cell transfection experiments were performed by Lipofectamine 2000 (Thermo fisher, USA) after one-day seeding.

2.4. Cell Viability. A549 cells were seeded on the surface of dielectric-elastomer membrane and 24-well plates; cells were incubated for 24 h, 36 h, and 48 h at 37 °C with 5% CO₂. Cell viability was determined using cell counting kit-8 (CCK-8, Yeasen, Shanghai, China), and absorbance was recorded on a microplate reader (Tecan Austria GmbH, Austria) at a wavelength of 450 nm.

2.5. Immunofluorescence Staining. To observe the change of cell morphology with membrane tension, F-actin of A549 cells on the dielectric-elastomer membrane was stained with Alexa Fluor 488 phalloidin (Cell Signaling Technology, USA) for 1 h, and nuclei were stained with DAPI for 10 min. The staining cells were stretched at an electric field of 140 V/ μm and observed with a fluorescence microscope.

2.6. EGFP Transfection. About 24 h later, when the cell density reached about 70–80%, the DEA-based deformable bioreactor was transferred into the designed cell culture device for transfection experiments. A Lipofectamine 2000 (lipo-2000) transfection reagent was used to represent the lipofection technique, which can use the positive surface charge of the liposomes to interact with the negatively charged cell membrane and mediate the plasmid into cells. Cells were

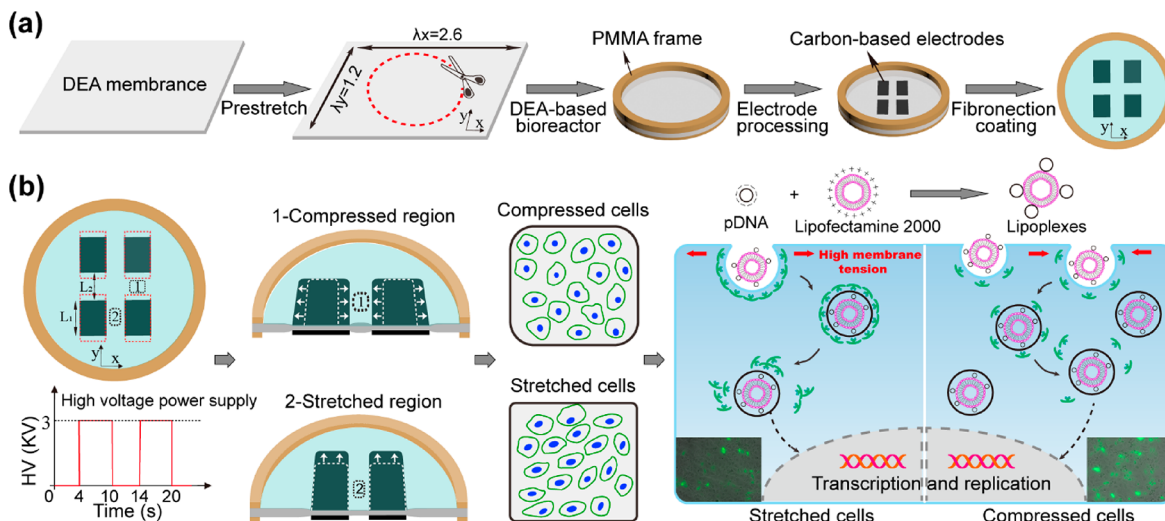


Figure 1. Preparation and schematic diagram of the DEA-based bioreactor. (a) Preparation of the DEA-based bioreactor. (b) Working principle of the DEA-based bioreactor and the effect of mechanical stimulation to EGFP transfection efficiency.

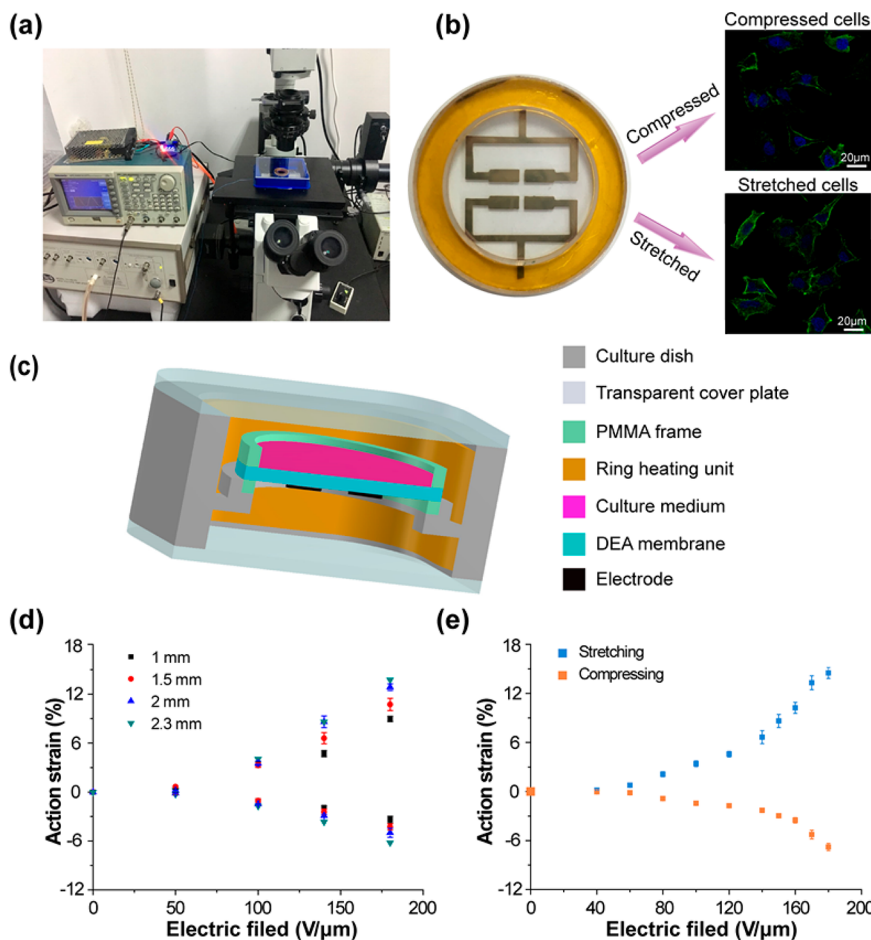


Figure 2. Experimental setup and characterization of DEA-based bioreactor system. (a) DEA-based bioreactor was placed on an inverted microscope for real-time observation of cell membrane tension. (b) Stained cytoskeleton and nucleus were imaged by confocal microscope to observe the cell morphology, and the images were tested after 12 h of cyclic stimulation with 0.1 Hz sinusoidal wave. (c) Three-dimensional assembly diagram of DEA-based bioreactor. (d) Average strain of the dielectric elastomer membrane at different electrode spacings along the electrode stretching direction. (e) Average strain in the stretching and compressing regions; electrode spacing along the electrode stretching direction was 2 mm.

seeded in the DEA-based bioreactor and cultured in Dulbecco's modified Eagle's medium (DMEM) containing 10% fetal bovine

serum (FBS) without antibiotics before transfection. When the cells obtained 70–80%, lipo-2000 and plasmid were mixed with Opti-

MEM medium (Gibco, USA), respectively, and incubated for 5 min at room temperature, the ratio of plasmid (μg) to lipo-2000 (μL) was 1:2. Six microliters of lipo-2000 was combined with 150 μL of Opti-MEM medium and 3 μg of plasmid with 150 μL of Opti-MEM medium. Then the two solutions were mixed and incubated for 15 min. Finally, the complexes were added to the growth medium (1 mL for each well). The transfection was carried out at 37 °C for 10 min, and then the transfection-medium was removed and replaced with fresh growth media containing 10% FBS and 1% penicillin/streptomycin (Gibco, USA). The transfection results were detected using an inverted fluorescence microscope after 1 day.

2.7. Effect of Fringing Electric Field. We selected the nondielectric elastomer membrane to repeat the electric field stimulation test. Two different electric field intensities, 100 $\text{V}/\mu\text{m}$ and 160 $\text{V}/\mu\text{m}$, were selected to demonstrate the effect of fringing electric field on transfection efficiency under a constant stimulus condition for 10 min (10 mHz, 100% duty cycle).

2.8. Effect of Mechanical Stimulation on Gene Expression and Endocytosis Inhibition Assay of pDNA. We changed the order of mechanical stimulation and lipoplexes endocytosis. First of all, in the static environment, the cells in the experimental groups and the control group were incubated with the same concentration of lipoplexes for 10 min, and then the transfection-medium was removed and replaced with fresh 10% FBS+/1% antibiotics+ medium. The cells in the experimental group were mechanically stimulated after endocytosis, and the control group was cultured under the same static environment. The stretching ratio of dielectric-elastomer membrane was 4–8% at a 10 mHz frequency with a 100% duty cycle.

After that, the endocytosis way of lipoplexes in A549 cells was verified. The A549 cells were pretreated with chlorpromazine, genistein, and wortmannin for 30 min at 37 °C, which can inhibit the endocytosis pathway mediated by clathrin, caveolin, and macrocytosis, respectively. Then the transfection reagent was added and incubated for 1 h. The inhibitory effect of each pathway was analyzed 24 h later for EGFP expression.

2.9. Gene Transfection Efficiency Assays. An inverted fluorescence imaging microscopy was used to observe and image the EGFP expression. Ten different regions were selected for imaging statistics in each stimulation regions, and the bright field and fluorescence maps for each area were collected. The total number of cells and the number of cells expressed green fluorescence in the region were counted by ImageJ software. Thus, the efficiency of gene transfection was calculated and compared. For plotting the transfection efficiency, origin software was used to normalized all data to the mean value of the static control group. A box plot was drawn to represent the differences between groups; it covers 25% to 75% of data points and contains median and standard deviation. The total number of cells in each group was also marked in the figure. The statistical significance for the differences of the transfection efficiency under different stimulation conditions was established using the Mann–Whitney test and p values was used to determine the significance ($p < 0.001$).

3. RESULTS AND DISCUSSION

3.1. Preparation and Characterization of DEA-Based Bioreactor. The fabrication process of DEA-based bioreactor was shown in Figure 1a. To decrease the exciting voltage of the DEA, the first step to fabricate the DEA-based bioreactor was to prestretch the dielectric-elastomer membrane.^{35,36} Meanwhile, the stretching ratio in x -axis was twice that of the y -axis, resulting in higher stiffness of x axis than that of y axis, and the membrane tended to move in the y direction under high voltage. Then the prestretched silicone membrane was fixed on the PMMA frame. Different electrode arrays can achieve different movements,^{38,40} and we designed a four-electrode DEA-based bioreactor to realize the stretching and compression deformation on a membrane simultaneously. Finally, the substrate was coated with fibronectin to improve the

biocompatibility of the silicone membrane substrate and facilitate cell adhesion. The working principle of DEA-based bioreactor was shown in Figure 1b, under the action of electric field, the transparent region 2 was stretched with the movement of the electrode region, while the region 1 between the two electrodes was compressed due to the squeezing of electrodes on both sides. In addition, a high-throughput cell incubator was designed to carry out four groups of cell transfection tests at the same time (Figure S1). In summary, the DEA-based bioreactor not only enabled stretching and compressing movements on a membrane but also ensured the visualization of the stimulation area, which was beneficial to observe the test results.

Figure 2a shows a cell culture device integrated with a DEA-based bioreactor, which could be perfectly integrated with a fluorescence microscope and the state of cells could be observed in real time under the mechanical stimulation. To demonstrate the effect of mechanical stimulation on cells morphology, the cells were stimulated for 12 h with 0.1 Hz, and cytoskeleton staining results showed that the aspect ratios of the cytoskeleton in the stretched and compressed regions were different (Figure 2b). Three-dimensional assembly diagram of the DEA-based bioreactor was shown in Figure 2c; the device was mainly composed of a cell culture device and a DEA-based bioreactor, which could be used to study the effect of mechanical stimulation on adherent cells biological behavior. First, due to the high environmental requirements for cell growth, we measured the temperature distribution in the culture device (Figure S2), the temperature distribution around the culture dish was uniform, and the temperature fluctuation of each point was small within 2 h, which fully met the necessary temperature requirements for cell growth.

In addition, the average strain of the membrane was characterized by tracking the edge displacement of the electrodes using microscope (Figure 2d,e). Because of the modus of multielectrode driving, the electrodes spacing has great influence on the performance of the actuators, especially to the driving direction. Therefore, we designed four DEAs with different electrode spacings, and the membranes performance was shown in Figure 2d; the interference between the electrodes was obvious when the electrode spacing was less than 1.5 mm, and the tensile properties of the membrane were significantly suppressed. In contrast, the driving performance of the membrane tended to be stable with the electrode spacing of 2 mm (Figure 2e). The blue curve represents the average deformation of the stretching region, and the orange curve represents the average strain in the compressing region between the two electrodes. Overall, under the same electric field, the deformation of the stretching region was greater than that of the compressing region. For example, when an electric field of 170 $\text{V}/\mu\text{m}$ was applied, the average strain in stretching region was 13% but only about 6% of the compressing region. At the same time, due to the limitations of electrodes design and the membrane characteristics, the deformation degree of the membrane was different in different regions.^{38,41–43} For the rigor of the experiment, the displacement of the membrane was measured at 140 $\text{V}/\mu\text{m}$ (Figure S3). In the center of stimulation region, the deformation fluctuation of the DE membrane was about 1%, indicating that the uniform deformation could be used for experimental research. The experimental data were also selected at the uniform strain area.

The biocompatibility of dielectric-elastomer membrane was evaluated using CCK-8 assay, and cell viability still was

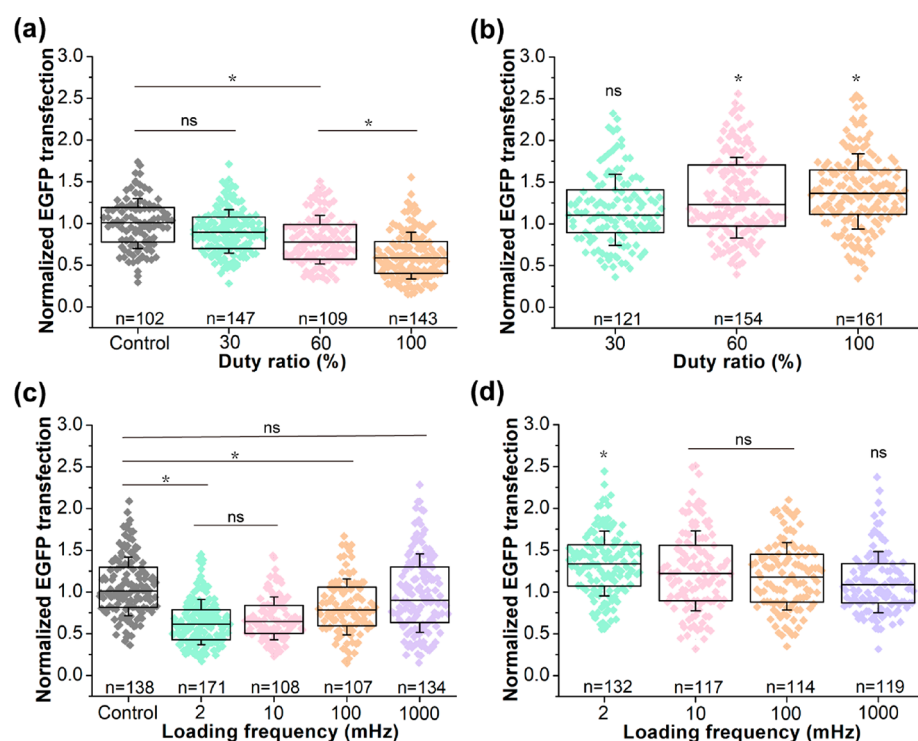


Figure 3. Effect of duty ratio and loading frequency on EGFP transfection efficiency. (a) Effect of duty ratio on EGFP transfection efficiency of stretching regions. (b) Effect of duty ratio on EGFP transfection efficiency of compressing regions. (c) Effect of loading frequency on EGFP transfection efficiency of stretching regions. (d) Effect of loading frequency on EGFP transfection efficiency of compressing regions. A box plot is drawn to represent the median and standard deviation, and it covers 25% to 75% of data points. The “n” represents the total number of regions used to calculate transfection efficiency. *, $p < 0.001$; “ns” represents not significant between the comparison groups.

maintained above 90% compared with the 24-well plate after 48 h (Figure S4), which demonstrated that the DEA-based bioreactor could be used for cell mechanical stimulation tests. Real-time imaging photos showed the deformation of the cytoskeleton during mechanical stimulation (Figure S5); the merged images clearly showed that the cells were stretched and compressed with the changes of dielectric-elastomer membrane at an electric field of $140 \text{ V}/\mu\text{m}$.

3.2. Effect of Duty Ratio and Loading Frequency on EGFP Transfection Efficiency. A549 cells were cultured on the surface of DEA membrane for 24 h and then transfected with EGFP plasmid to investigate the influence of mechanical stimulation on gene transfection efficiency. The duty cycles we chose for test were 30%, 60%, and 100%, respectively. The results of EGFP transfection were shown in Figure 3a and b, with the same time of cell transfection; as the duty cycle increased, the inhibitory effect of EGFP transfection became more and more obvious. When the duty cycle was more than 60%, the transfection efficiency was no longer significantly changed; due to the relationship between the change of cell membrane tension and the time of vesicle transport, the action mechanism will be further explained in the following section. A similar phenomenon was also reflected in the compression group, and only when the duty cycle was large enough, the positive effect of compression on the cell transfection efficiency was manifested.

As an important parameter to change the way of mechanical stimulation, the loading frequency also affected the transfection efficiency of cells (Figure 3c,d). Under the stimulation of 1 Hz frequency, the transfection efficiency of cells in the stretching regions fluctuated more than that of the low-frequency regions. At the same time, the transfection efficiency under the

stretching stimulation of 1 Hz slightly decreased compared with the control group, but for the compressing regions, the transfection efficiency under a loading frequency of 1 Hz was not significantly different from that of the control group. With the decrease of loading frequency, the transfection efficiency of the stretching regions decreased gradually, and the transfection efficiency was only about 60% of the control group at 10 mHz frequency. The transfection efficiencies in compressing regions were similar at 10 mHz and 100 mHz, but the number of high expressed region cells was lower than that of 2 mHz. The results indicated that continuous and stable mechanical stimulation could promote or inhibit the cell transfection efficiency. In summary, changing the loading frequency or duty cycle will affect the times of cell membrane stretch release, and previous studies have revealed that the endocytosis of cell membrane significantly increased during the release of cell tension,^{26,44} the change of transfection efficiency caused by the loading frequency and duty cycle could be related to the mechanism, which has yet to be illustrated.

The mechanism of DEA was shown in Figure S6a, the membrane was extruded under the action of electric field, and the electric field was mainly distributed in the membrane thickness range and had no influence on the upper surface of the membrane. However, in the edge of electrodes, there was an electric field leakage and cells in the region were likely to be affected by electric field stimulation.⁴² To distinguish the effect of electric field and the mechanical stimulation, the effect of electric field on transfection efficiency was studied alone. As demonstrated in Figure S6b, the transfection efficiency of cells in observed regions was not influenced by the individual electric field, which indicated that the fringing electric field had no obvious effect on EGFP transfection efficiency in our test.

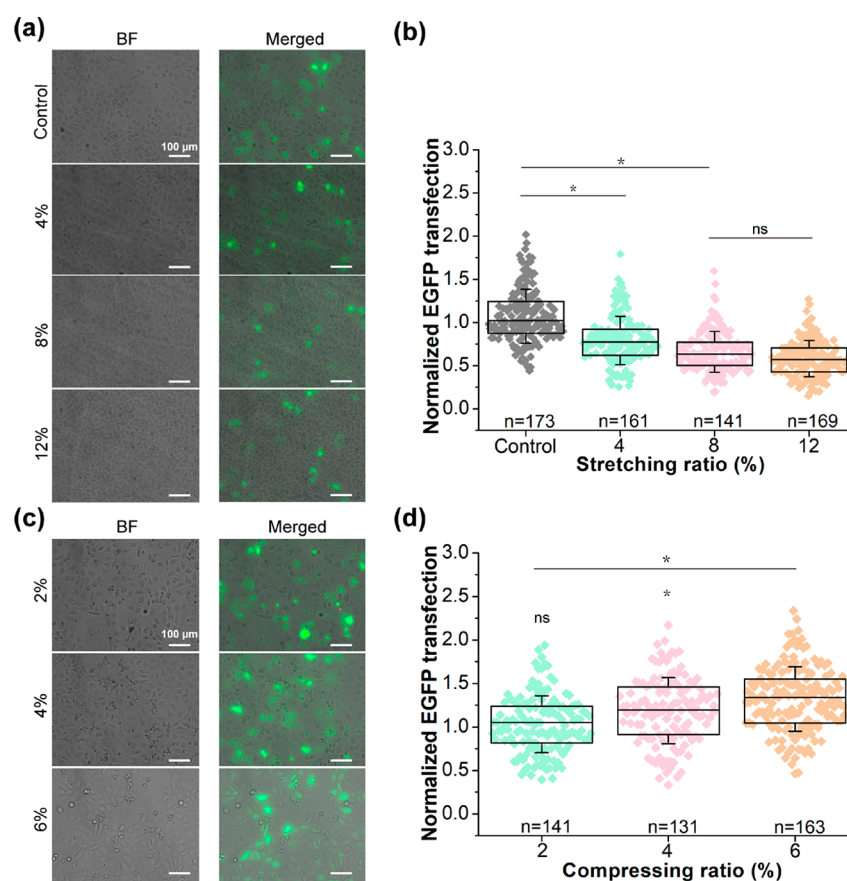


Figure 4. Effect of cell membrane tension on EGFP transfection efficiency. (a) Representative fluorescence images of bright field and EGFP (green) expression and (b) inhibitory effect of stretching ratios on EGFP transfection efficiency. (c) Representative fluorescence images of bright field and EGFP (green) expression and (d) promoting effect of compression ratios on EGFP transfection efficiency. A box plot is drawn to represent the median and standard deviation, and it covers 25% to 75% of data points. The “n” represents the total number of regions used to calculate transfection efficiency. *, $p < 0.001$; “ns” represents not significant between the comparison groups.

The details of fringing electric test can be found in the [Supporting Information](#).

3.3. Effect of Membrane Tension on EGFP Transfection Efficiency. The effect of the membrane tension on the transfection efficiency of the plasmid was tested with 0–12% stretching range and 0–6% compression range of membrane. Transfected cells were stimulated for 10 min at different stretching ratio and observed after 24 h, as shown in [Figure 4a](#). The normalized EGFP transfection results showed that the EGFP transfection efficiency is significantly lower than that of the control group in the stretching regions ([Figure 4b](#)). Moreover, with the increase of dielectric-elastomer membrane tension, the inhibitory effect on EGFP transfection efficiency was more obvious. When the membrane tension increased to 12%, the transfection efficiency of EGFP was only about 60% that of the control group, which fully demonstrated the increasing inhibitory effect of the membrane tension on the transfection efficiency. In contrast, an opposite conclusion was found in the compressing regions ([Figure 4c,d](#)); with the increase of compression ratio, the efficiency of EGFP transfection was higher than that of the control group. Specifically, when the compression strain was less than 2%, the efficiency of EGFP transfection did not change significantly. However, when the compression strain was more than 4%, the efficiency of EGFP transfection would gradually increase. It can also be seen that the distribution of transfection efficiency in the control group was scattered, but

the distribution was more concentrated in the stimulated regions, which further verify the effect of mechanical stimulation on gene transfection. The above results demonstrated that the increase of membrane tension led to a decrease of EGFP transfection efficiency; this was also consistent with previous reports,^{26,44} while cells in the compressing regions showed high EGFP expression. As reported in previous works, mechanical stimulation has influence on cell endocytosis especially mediated by clathrin.^{9,21,32} Moreover, the amount of plasmid complex endocytosis has been demonstrated as an important factor affecting the gene transfection efficiency,^{45–47} which implied that cellular endocytosis in DEA-based bioreactor was influenced by the change of membrane tension.

3.4. Analysis of Factors Affecting Transfection Efficiency by Mechanical Stimulation. Transfection is the process of actively introducing DNA into the cell. In general, the EGFP transfection process can be divided into two stages, the uptake of the plasmid and the process of transferring plasmid DNA into the nucleus and expression. The results showed that mechanical stimulation can affect the EGFP transfection efficiency, but the specific influence factors need to be further investigated. Thus, we tested the effect of mechanical stimulation on pDNA expression after cells endocytosis. As presented in [Figure 5](#), the cells were cultured with lipoplexes for 10 min in a static state and then stimulated after replaced with normal medium. Compared with the control group, the EGFP transfection efficiency of the

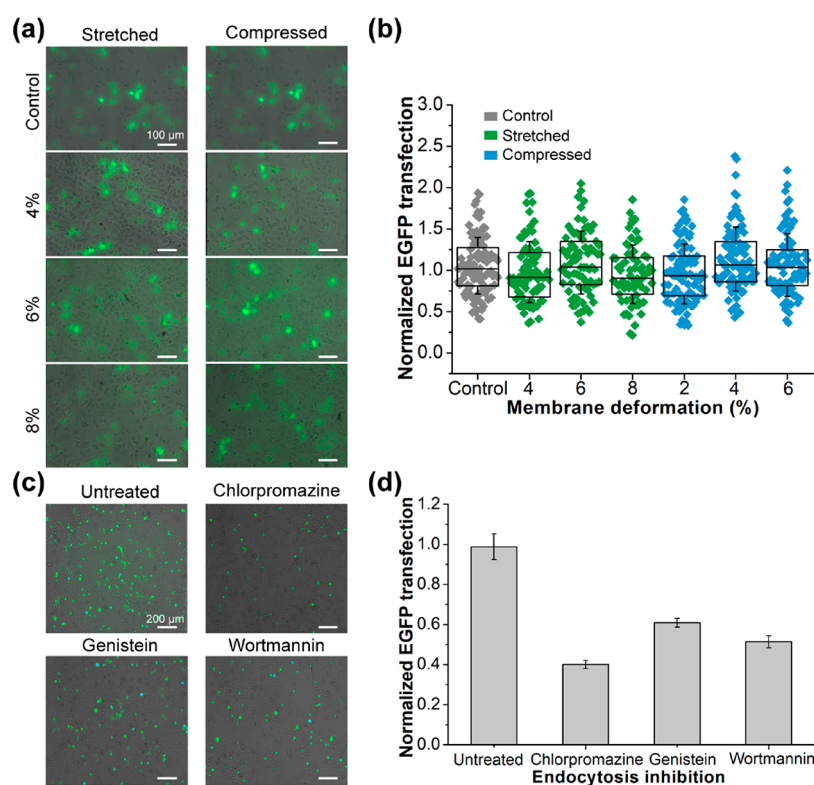


Figure 5. Analysis of factors affecting transfection efficiency by mechanical stimulation. (a) Representative fluorescence images of EGFP (green) expression. (b) Quantitative analysis of the effect of mechanical stimulations on transfection efficiency after cells endocytosis. (c) Representative fluorescence images of EGFP (green) expression and (d) analysis of relative transfection efficiency after the inhibition of specific pathways by endocytosis inhibitors.

stretched group fluctuated slightly under the stretching stimulation of 4–8%, implying that there was no obvious inhibition of transfection efficiency (Figure 5a,b). The same results were also found in the compression group; even at 6% compression stimulation, transfection efficiency was not different from the control group, and there was no tendency to show a significant increase in the amount of high expression. It should be noted that the elastic modulus of the cell culture substrate affects the force transfer between the cell membrane and the nucleus.^{48–50} For cells grown on a silicone membrane substrate in this experiment, mechanical stimulation did not significantly affect the plasmid entry into the nucleus and subsequent expression after endocytosis. The results showed that the effect of mechanical stimulation on EGFP transfection efficiency was mainly due to the first stage of cell endocytosis.

To investigate the endocytosis pathway of lipoplexes in A549 cells, three main pathways of endocytosis in A549 cells were studied in this work: clathrin-, caveolae-, and macropinocytosis-mediated endocytosis pathways were inhibited by chlorpromazine HCl, genistein, and wortmannin, respectively. As show in Figure S7, the transfection efficiency of EGFP decreased when the three pathways were inhibited, indicating that the endocytosis of lipoplexes was related to all three endocytosis pathways. Furthermore, the clathrin-mediated pathway had an obvious inhibitory effect with less than 40% EGFP expression relative to the control group (Figure 5c,d), which proved that the clathrin-mediated pathway plays a leading role in uptake of lipoplexes in A549 cells. Previous studies have revealed that membrane tension has an effect on the formation of clathrin coated pits,³¹ which will affect the cell endocytosis. Thus, we hypothesize that the change of

membrane tension caused by DEA mainly affected the formation of vesicles, thereby affecting the endocytosis of lipoplexes and EGFP transfection efficiency, which has yet to be illustrated.

4. CONCLUSION

DEA-based bioreactors were successfully applied to precisely control the mechanical stimulation of A549 cells. On the basis of the dynamic stimulation bioreactor, A549 cells were incubated to investigate the influence of stretching and compressing stimulation on EGFP transfection efficiency. We demonstrated that on silicone membrane, the effect of mechanical stimulation on cells gene transfection efficiency was mainly due to the effect of membrane tension on cell endocytosis. The transfection efficiency of cells decreased under stretching stimulation, indicating that the increase of membrane tension has an inhibitory effect on EGFP transfection. On the contrary, transfection efficiency of cells tended to increase in compressing regions. Similarly, the frequency and duration of cell membrane tension release also influence the transfection efficiency of cells, which could be controlled by parameters such as duty cycle and loading frequency. The results should provide a research idea for improving the efficiency of gene transfection.

■ ASSOCIATED CONTENT

Supporting Information

The Supporting Information is available free of charge at <https://pubs.acs.org/doi/10.1021/acsabm.9b01199>.

Temperature distribution in the culture device; picture and exploded view of high-throughput cell incubator;

deformation distribution of membrane; cell viability cultured on the dielectric-elastomer membrane; deformation of cells under mechanical stimulation; effect of fringing electric field on EGFP transfection efficiency; endocytosis inhibition assay (PDF)

AUTHOR INFORMATION

Corresponding Authors

Guoying Gu – Robotics Institute, School of Mechanical Engineering, Shanghai Jiao Tong University, Shanghai 200240, People's Republic of China; Email: guguoying@sjtu.edu.cn

Wei Tao – Institute of Nano Biomedicine and Engineering, Department of Instrument Science and Engineering, School of Electronic Information and Electrical Engineering, Shanghai Jiao Tong University, Shanghai 200240, People's Republic of China; Email: taowei@sjtu.edu.cn

Jie Song – Institute of Nano Biomedicine and Engineering, Department of Instrument Science and Engineering, School of Electronic Information and Electrical Engineering, Shanghai Jiao Tong University, Shanghai 200240, People's Republic of China; Institute of Cancer and Basic Medicine (ICBM), Chinese Academy of Sciences; The Cancer Hospital of the University of Chinese Academy of Sciences, Hangzhou 310022, People's Republic of China; orcid.org/0000-0002-4711-6014; Email: sjie@sjtu.edu.cn

Authors

Chao Gao – Institute of Nano Biomedicine and Engineering, Department of Instrument Science and Engineering, School of Electronic Information and Electrical Engineering, Shanghai Jiao Tong University, Shanghai 200240, People's Republic of China

Zhichao Li – Institute of Nano Biomedicine and Engineering, Department of Instrument Science and Engineering, School of Electronic Information and Electrical Engineering, Shanghai Jiao Tong University, Shanghai 200240, People's Republic of China

Jiang Zou – Robotics Institute, School of Mechanical Engineering, Shanghai Jiao Tong University, Shanghai 200240, People's Republic of China

Jin Cheng – Institute of Nano Biomedicine and Engineering, Department of Instrument Science and Engineering, School of Electronic Information and Electrical Engineering, Shanghai Jiao Tong University, Shanghai 200240, People's Republic of China

Kai Jiang – Institute of Nano Biomedicine and Engineering, Department of Instrument Science and Engineering, School of Electronic Information and Electrical Engineering, Shanghai Jiao Tong University, Shanghai 200240, People's Republic of China

Changrun Liu – Institute of Nano Biomedicine and Engineering, Department of Instrument Science and Engineering, School of Electronic Information and Electrical Engineering, Shanghai Jiao Tong University, Shanghai 200240, People's Republic of China

Complete contact information is available at:
<https://pubs.acs.org/10.1021/acsabm.9b01199>

Author Contributions

[†]C.G., Z.L., and J.Z. contributed equally.

Notes

The authors declare no competing financial interest.

ACKNOWLEDGMENTS

The authors are grateful for the financial support from the National Natural Science Foundation of China (Nos. 81822024, 11761141006), the Natural Science Foundation

of Shanghai, China (Nos. 19520714100, 19ZR1475800), the National Key Research and Development Program of China (Grant No. 2017YFC1200904), and the Medical Engineering Cross Project of Shanghai Jiaotong University (YG2017ZD07).

REFERENCES

- (1) Wang, C. H.; Pun, S. H. Substrate-mediated nucleic acid delivery from self-assembled monolayers. *Trends Biotechnol.* **2011**, *29*, 119–126.
- (2) Zeitelhofer, M.; Vessey, J. P.; Xie, Y.; Tubing, F.; Thomas, S.; Kiebler, M.; Dahm, R. High-efficiency transfection of mammalian neurons via nucleofection. *Nat. Protoc.* **2007**, *2*, 1692–1704.
- (3) Wang, Y.; Zhao, S.; Bai, L.; Fan, J.; Liu, E. Expression systems and species used for transgenic animal bioreactors. *BioMed Res. Int.* **2013**, *2013*, 580463.
- (4) Wang, J.; Ren, K.-F.; Gao, Y.-F.; Zhang, H.; Huang, W.-P.; Qian, H.-L.; Xu, Z.-K.; Ji, J. Photothermal spongy film for enhanced surface-mediated transfection to primary cells. *ACS Applied Bio Materials.* **2019**, *2*, 2676–2684.
- (5) Dunbar, C. E.; High, K. A.; Joung, J. K.; Kohn, D. B.; Ozawa, K.; Sadelain, M. Gene therapy comes of age. *Science* **2018**, *359*, eaan4672.
- (6) McMahon, M. A.; Cleveland, D. W. Gene therapy: Gene-editing therapy for neurological disease. *Nat. Rev. Neurol.* **2017**, *13*, 7–9.
- (7) Liu, Y.; Yan, J.; Santangelo, P. J.; Prausnitz, M. R. DNA uptake, intracellular trafficking and gene transfection after ultrasound exposure. *J. Controlled Release* **2016**, *234*, 1–9.
- (8) Lechardeur, D.; Sohn, K.-J.; Haardt, M.; Joshi, P.; Monck, M.; Graham, R.; Beatty, B.; Squire, J.; Brodovich, H. O.; Lukacs, G. Metabolic instability of plasmid DNA in the cytosol: a potential barrier to gene transfer. *Gene Ther.* **1999**, *6*, 482–497.
- (9) Mettlen, M.; Chen, P. H.; Srinivasan, S.; Danuser, G.; Schmid, S. L. Regulation of clathrin-mediated endocytosis. *Annu. Rev. Biochem.* **2018**, *87*, 871–896.
- (10) Begley, C. M.; Kleis, S. J. The fluid dynamic and shear environment in the NASA/JSC rotating-wall perfused-vessel bioreactor. *Biotechnol. Bioeng.* **2000**, *70*, 32–40.
- (11) Piret, J. M.; Cooney, C. L. Model of oxygen transport limitations in hollow fiber bioreactors. *Biotechnol. Bioeng.* **1991**, *37*, 80–92.
- (12) Madeira, C.; Mendes, R. D.; Ribeiro, S. C.; Boura, J. S.; Aires-Barros, M. R.; da Silva, C. L.; Cabral, J. M. Nonviral gene delivery to mesenchymal stem cells using cationic liposomes for gene and cell therapy. *J. Biomed. Biotechnol.* **2010**, *2010*, 735349.
- (13) Wu, T.; Li, Z.; Zhang, Y.; Ji, J.; Huang, Y.; Yuan, H.; Feng, F.; Schanze, K. S. Remarkable amplification of polyethylenimine-mediated gene delivery using cationic poly(phenylene ethynylene)s as photosensitizers. *ACS Appl. Mater. Interfaces* **2018**, *10*, 24421–24430.
- (14) Liu, T.; Tang, A.; Zhang, G.; Chen, Y.; Zhang, J.; Peng, S.; Cai, Z. Calcium phosphate nanoparticles as a novel nonviral vector for efficient transfection of DNA in cancer gene therapy. *Cancer Biother. Radiopharm.* **2005**, *20*, 141–149.
- (15) Rubinson, D. A.; Dillon, C. P.; Kwiatkowski, A. V.; Sievers, C.; Yang, L.; Kopinja, J.; Rooney, D. L.; Zhang, M.; Ihrig, M. M.; McManus, M. T.; Gertler, F. B.; Scott, M. L.; Van Parijs, L. A lentivirus-based system to functionally silence genes in primary mammalian cells, stem cells and transgenic mice by RNA interference. *Nat. Genet.* **2003**, *33*, 401–406.
- (16) Naldini, L.; Blomer, U.; Galloway, P.; Ory, D.; Mulligan, R.; Gage, F. H.; Verma, I. M.; Trono, D. In vivo gene delivery and stable transduction of nondividing cells by a lentiviral vector. *Science* **1996**, *272*, 263–267.
- (17) Mellott, A. J.; Forrest, M. L.; Detamore, M. S. Physical non-viral gene delivery methods for tissue engineering. *Ann. Biomed. Eng.* **2013**, *41*, 446–468.

- (18) Covello, G.; Siva, K.; Adami, V.; Denti, M. A. An electroporation protocol for efficient DNA transfection in PC12 cells. *Cytotechnology* **2014**, *66*, 543–453.
- (19) Yang, Y.; Wang, X.; Hu, X.; Kawazoe, N.; Yang, Y.; Chen, G. Influence of cell morphology on mesenchymal stem cell transfection. *ACS Appl. Mater. Interfaces* **2019**, *11*, 1932–1941.
- (20) Batchelder, E. L.; Hollopeter, G.; Campillo, C.; Mezanges, X.; Jorgensen, E. M.; Nassoy, P.; Sens, P.; Plastino, J. Membrane tension regulates motility by controlling lamellipodium organization. *Proc. Natl. Acad. Sci. U. S. A.* **2011**, *108*, 11429–11434.
- (21) Holst, M. R.; Vidal-Quadras, M.; Larsson, E.; Song, J.; Hubert, M.; Blomberg, J.; Lundborg, M.; Landstrom, M.; Lundmark, R. Clathrin-independent endocytosis suppresses cancer cell blebbing and invasion. *Cell Rep.* **2017**, *20*, 1893–1905.
- (22) Kim, J. H.; Ren, Y.; Ng, W. P.; Li, S.; Son, S.; Kee, Y. S.; Zhang, S.; Zhang, G.; Fletcher, D. A.; Robinson, D. N.; Chen, E. H. Mechanical tension drives cell membrane fusion. *Dev. Cell* **2015**, *32*, 561–573.
- (23) Pontes, B.; Monzo, P.; Gauthier, N. C. Membrane tension: A challenging but universal physical parameter in cell biology. *Semin. Cell Dev. Biol.* **2017**, *71*, 30–41.
- (24) Yoshida, A.; Sakai, N.; Uekusa, Y.; Imaoka, Y.; Itagaki, Y.; Suzuki, Y.; Yoshimura, S. H. Morphological changes of plasma membrane and protein assembly during clathrin-mediated endocytosis. *PLoS Biol.* **2018**, *16*, e2004786.
- (25) Diz-Munoz, A.; Fletcher, D. A.; Weiner, O. D. Use the force: membrane tension as an organizer of cell shape and motility. *Trends Cell Biol.* **2013**, *23*, 47–53.
- (26) Thottacherry, J. J.; Kosmalska, A. J.; Kumar, A.; Vishen, A. S.; Elosegui-Artola, A.; Pradhan, S.; Sharma, S.; Singh, P. P.; Guadamillas, M. C.; Chaudhary, N.; Vishwakarma, R.; Trepast, X.; Pozo, M. A. D.; Parton, R. G.; Rao, M.; Pullarkat, P.; Roca-Cusachs, P.; Mayor, S. Mechanochemical feedback control of dynamin independent endocytosis modulates membrane tension in adherent cells. *Nat. Commun.* **2018**, *9*, 4217.
- (27) Keren, K.; Pincus, Z.; Allen, G. M.; Barnhart, E. L.; Marriott, G.; Mogilner, A.; Theriot, J. A. Mechanism of shape determination in motile cells. *Nature* **2008**, *453*, 475–480.
- (28) Picco, A.; Kukulski, W.; Manenschijn, H. E.; Specht, T.; Briggs, J. A. G.; Kaksonen, M. The contributions of the actin machinery to endocytic membrane bending and vesicle formation. *Mol. Biol. Cell* **2018**, *29*, 1346–1358.
- (29) Keren, K. Membrane tension leads the way. *Proc. Natl. Acad. Sci. U. S. A.* **2011**, *108*, 14379–14380.
- (30) Giannone, G.; Dubin-Thaler, B. J.; Rossier, O.; Cai, Y.; Chaga, O.; Jiang, G.; Beaver, W.; Dobereiner, H. G.; Freund, Y.; Borisy, G.; Sheetz, M. P. Lamellipodial actin mechanically links myosin activity with adhesion-site formation. *Cell* **2007**, *128*, 561–575.
- (31) Boulant, S.; Kural, C.; Zeeh, J. C.; Ubelmann, F.; Kirchhausen, T. Actin dynamics counteract membrane tension during clathrin-mediated endocytosis. *Nat. Cell Biol.* **2011**, *13*, 1124–1131.
- (32) Senju, Y.; Lappalainen, P. Regulation of actin dynamics by PI(4,5)P2 in cell migration and endocytosis. *Curr. Opin. Cell Biol.* **2019**, *56*, 7–13.
- (33) Mund, M.; Beek, J. A. v. d.; Deschamps, J.; Dmitrieff, S.; Hoess, P.; Monster, J. L.; Picco, A.; Nedelec, F.; Kaksonen, M.; Ries, J. Systematic nanoscale analysis of endocytosis links efficient vesicle formation to patterned actin nucleation. *Cell* **2018**, *174*, 884–896.
- (34) Li, Z.; Gao, C.; Fan, S.; Zou, J.; Gu, G.; Dong, M.; Song, J. Cell nanomechanics based on dielectric elastomer actuator device. *Nano-Micro Lett.* **2019**, *11*, 98.
- (35) Koh, S. J. A.; Li, T.; Zhou, J.; Zhao, X.; Hong, W.; Zhu, J.; Suo, Z. Mechanisms of large actuation strain in dielectric elastomers. *J. Polym. Sci., Part B: Polym. Phys.* **2011**, *49*, 504–515.
- (36) Poulin, A.; Rosset, S.; Shea, H. Fabrication and characterization of silicone-based dielectric elastomer actuators for mechanical stimulation of living cells. *Electroactive Polymer Actuators and Devices (EAPAD)*. **2018**, 10594, 105940V.
- (37) Rosset, S.; Shea, H. R. Flexible and stretchable electrodes for dielectric elastomer actuators. *Appl. Phys. A: Mater. Sci. Process.* **2013**, *110*, 281–307.
- (38) Poulin, A.; Saygili Demir, C.; Rosset, S.; Petrova, T. V.; Shea, H. Dielectric elastomer actuator for mechanical loading of 2D cell cultures. *Lab Chip* **2016**, *16*, 3788–3794.
- (39) Blaber, J.; Adair, B.; Antoniou, A. Ncorr: open-source 2D digital image correlation matlab software. *Exp. Mech.* **2015**, *55*, 1105–1122.
- (40) Gu, G. Y.; Zhu, J.; Zhu, L. M.; Zhu, X. A survey on dielectric elastomer actuators for soft robots. *Bioinspir. Biomim.* **2017**, *12*, 011003.
- (41) Akbari, S.; Rosset, S.; Shea, H. More than 10-fold increase in the actuation strain of silicone dielectric elastomer actuators by applying prestrain. *Proc. SPIE* **2013**, 8687, 86871P.
- (42) Wang, N. F.; Cui, C. Y.; Guo, H.; Chen, B.; Zhang, X. M. Advances in dielectric elastomer actuation technology. *Sci. China: Technol. Sci.* **2018**, *61*, 1512–1527.
- (43) Gu, G.; Zou, J.; Zhao, R.; Zhao, X.; Zhu, X. Soft wall-climbing robots. *Science Robotics*. **2018**, *3*, eaat2874.
- (44) Dai, J.; Ting-Beall, H. P.; Sheetz, M. P. The secretion-coupled endocytosis correlates with membrane tension changes in RBL 2H3 cells. *J. Gen. Physiol.* **1997**, *110*, 1–10.
- (45) Ding, X.; Stewart, M.; Sharei, A.; Weaver, J. C.; Langer, R. S.; Jensen, K. F. High-throughput nuclear delivery and rapid expression of DNA via mechanical and electrical cell-membrane disruption. *Nat. Biomed Eng.* **2017**, *1*, 1–7.
- (46) Wang, P.-Y.; Lian, Y.-S.; Chang, R.; Liao, W.-H.; Chen, W.-S.; Tsai, W.-B. Modulation of PEI-mediated gene transfection through controlling cytoskeleton organization and nuclear morphology via nanogrooved topographies. *ACS Biomater. Sci. Eng.* **2017**, *3*, 3283–3291.
- (47) Gao, Y. G.; Alam, U.; Ding, A. X.; Tang, Q.; Tan, Z. L.; Shi, Y. D.; Lu, Z. L.; Qian, A. R. [12]aneN3-based lipid with naphthalimide moiety for enhanced gene transfection efficiency. *Bioorg. Chem.* **2018**, *79*, 334–340.
- (48) Elosegui-Artola, A.; Andreu, I.; Beedle, A. E. M.; Lezamiz, A.; Uroz, M.; Kosmalska, A. J.; Oria, R.; Kechagia, J. Z.; Rico-Lastres, P.; Le Roux, A. L.; Shanahan, C. M.; Trepast, X.; Navajas, D.; Garcia-Manyès, S.; Roca-Cusachs, P. Force triggers YAP nuclear entry by regulating transport across nuclear pores. *Cell* **2017**, *171*, 1397–1410.e14.
- (49) Elosegui-Artola, A.; Oria, R.; Chen, Y.; Kosmalska, A.; Perez-Gonzalez, C.; Castro, N.; Zhu, C.; Trepast, X.; Roca-Cusachs, P. Mechanical regulation of a molecular clutch defines force transmission and transduction in response to matrix rigidity. *Nat. Cell Biol.* **2016**, *18*, 540–548.
- (50) Lombardi, M. L.; Jaalouk, D. E.; Shanahan, C. M.; Burke, B.; Roux, K. J.; Lammerding, J. The interaction between nesprins and sun proteins at the nuclear envelope is critical for force transmission between the nucleus and cytoskeleton. *J. Biol. Chem.* **2011**, *286*, 26743–26753.